THE JOURNAL OF PHYSICAL CHEMISTRY B

Article

pubs.acs.org/JPCB

Ultrafast Studies of Excess Electrons in Liquid Acetonitrile: Revisiting the Solvated Electron/Solvent Dimer Anion Equilibrium

Stephanie C. Doan and Benjamin J. Schwartz*

Department of Chemistry and Biochemistry, University of California, Los Angeles, Los Angeles, California 90095, United States

Supporting Information

ABSTRACT: We examine the ultrafast relaxation dynamics of excess electrons injected into liquid acetonitrile using air- and water-free techniques and compare our results to previous work on this system [Xia, C. et al. *J. Chem. Phys.* **2002**, *117*, 8855]. Excess electrons in liquid acetonitrile take on two forms: a "traditional" solvated electron that absorbs in the near-IR, and a solvated molecular dimer anion that absorbs weakly in the visible. We find that excess electrons initially produced via charge-transfer-to-solvent excitation of iodide prefer to localize as solvated electrons, but that there is a subsequent equilibration to form the dimer anion on an ~80 ps time scale. The spectral signature of this interconversion between the two forms of the excess electron is a clear isosbestic point. The presence of the isosbestic point makes it possible to fully deconvolute the spectra of the two species. We find that solvated molecular anion absorbs quite weakly, with a maximum extinction coefficient of ~2000 $M^{-1}cm^{-1}$. With the extinction coefficient of the dimer anion in hand, we are also able to determine the equilibrium constant for the two forms of excess electron, and find that the molecular anion is favored by a factor of ~4. We also find that relatively little geminate recombination takes place, and that the geminate recombination that does take place is essentially complete within the first 20 ps. Finally, we show that the presence of small amounts of water in the acetonitrile can have a fairly large effect on the observed spectral dynamics, explaining the differences between our results and those in previously published work.

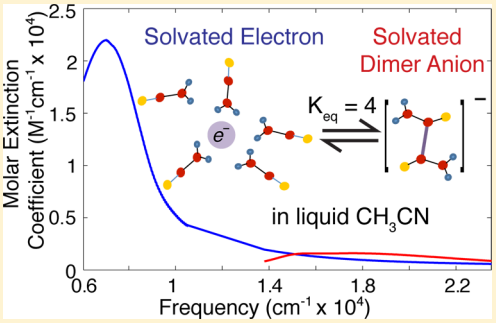

INTRODUCTION

Solvated electrons have been the focus of great interest because they provide for a direct comparison between the results of quantum simulations and ultrafast spectroscopic experiments. Although most of the focus has been on hydrated electrons,[1−4] solvated electrons also have been studied in many other solvents.[5−11] Of particular interest is the behavior of excess electrons in liquid acetonitrile (CH_3CN), a solvent with similar polarity and solvation dynamics to water.[12−15] Unlike water, when gas-phase molecules of CH_3CN bend, their electron affinity increases, so that a molecular anion can be stabilized in which the excess electron forms a covalent bond between the cyano-carbons of two bent, antiparallel CH_3CN molecules. Thus, when excess electrons are introduced into liquid CH_3CN, two species are formed.[16−22] One of these species has an absorption spectrum in the near-IR (NIR) that is identical to that of solvated electrons in solvents with similar polarity,[23] and this species has been assigned to be a typical dipole-bound solvated electron. The assignment of the other species, which absorbs weakly in the visible region of the spectrum, has been controversial, but current consensus suggests that this entity is a solvent-stabilized valence-bound CH_3CN molecular dimer anion.[18,19,21,22]

The idea that there are two excess electron species in liquid CH_3CN is also consistent with more recent studies on gas-phase $(CH_3CN)_n^-$ cluster anions. Mitsui et al. first observed excess electron species in $(CH_3CN)_n^-$ clusters with n = 10−100 with two distinct electron binding energies.[20] These researchers found that for smaller cluster sizes ($n \leq 12$), the species with lower binding energy predominates, and as cluster size grows, the species with higher binding energy becomes more prevalent.[20] Density functional theory-based quantum chemistry calculations on the smaller $(CH_3CN)_n^-$ clusters ($n \leq 10$) also supported the existence of two distinct excess electron species as well as the assignment of the more deeply bound species to the antiparallel bent structure of the dimer anion.[21,22] Time-resolved photoelectron spectroscopy (TRPES) experiments by Neumark and co-workers also found a greater population of the weakly bound species for small $(CH_3CN)_n^-$ clusters and more of the deeply bound species in larger clusters.[24−26] In addition, these workers noted that for larger cluster sizes, a lack of observed size dependence of the binding energy of the more deeply bound species is consistent with a highly localized excess electron that is not affected by CH_3CN molecules outside the first solvation shell.[26]

One of the central questions concerning the two excess electron species in liquid CH_3CN is the nature of the relationship between them. Kohler and co-workers addressed this question by performing ultrafast transient absorption

Special Issue: Paul F. Barbara Memorial Issue

Received: April 13, 2012
Revised: July 2, 2012
Published: July 5, 2012

   dx.doi.org/10.1021/jp303591h | *J. Phys. Chem. B* 2013, 117, 4216−4221

experiments examining excess electrons injected into liquid CH_3CN following excitation of the charge-transfer-to-solvent (CTTS) band of iodide.[18] These researchers found that both excess electron species were produced instantaneously upon excitation of iodide, and that the NIR-absorbing species was produced in excess of the visible-absorbing species. Kohler and co-workers found that the population of the NIR-absorbing species decayed in time, while that of the visible-absorbing species rose concomitantly. On the basis of these and other observations, these workers concluded that the visible species was a solvated dimer anion, and that this species was in equilibrium with the more traditional solvated electron species with an interconversion time scale of ∼260 ps. Around the same time, Shkrob and Sauer used a combination of mobility measurements and proton scavenging reactions to reach very similar conclusions.[19] Neither of these groups, however, were able to determine whether the weaker absorption of the solvated dimer anion species resulted from disfavorment of this species at equilibrium, or from an intrinsically low absorption cross-section.

In this paper, we revisit the ultrafast formation and interconversion dynamics of the excess electron species in liquid CH_3CN. Our work goes beyond the previous studies of Kohler and co-workers[18] in that our liquid CH_3CN sample is held in a rigorously air- and water-free environment and that we used a broadband probe pulse to collect complete spectra in the visible and NIR spectral ranges. With these advantages, we find a distinct isosbestic point during the interconversion of the two excess electron species, which in turn allows us to rigorously assign molar extinction coefficients for the two species. Our results show that the absorption cross-section of the solvated dimer anion is quite weak, and that the dimer anion is favored at equilibrium by a factor of ∼4 relative to the NIR-absorbing solvated electron. We also show that the presence of small amounts of water in liquid CH_3CN (which is highly hygroscopic) can affect both the interconversion and recombination dynamics of the two excess electron species.

EXPERIMENTAL METHODS

The femtosecond pump−probe spectrometer used in these experiments has been described in detail elsewhere.[27] Briefly, a Ti:Sapphire amplifier (Coherent, Legend Elite) is seeded with a broadband Ti:Sapphire oscillator (Coherent, Mantis). The amplifier output (35 fs, 3.2 mJ pulses at 800 nm with a 1 kHz repetition rate) was split into two beams of roughly equivalent power. Pump pulses at 266-nm with 25−35 μJ of energy for exciting the CTTS band of iodide were generated using a "double-mixing" scheme in which part of the beam is split off and doubled in a Type I β-barium borate (BBO) crystal, and the resultant 400-nm light is combined with the remaining 800 nm light in a second Type II BBO crystal. Broadband probe pulses in the visible (420−750 nm) were made by focusing a small portion of the 800 nm fundamental into a sapphire plate, while NIR white light (850−1650 nm) is made by focusing into a proprietary crystal plate (Ultrafast Systems, Helios). Measurements were taken by overlapping the pump and probe pulses on a 2 mm optical path-length spectrophotometric flow cell. The flow cell lines were kept air free and pumped at a rate that ensured a fresh sample volume for each pump pulse. Visible and NIR detector arrays were used for each respective measurement, collecting the full spectrum at each time point. All of the measurements were performed at room temperature.

In all of the transient absorption data presented below, we did not correct or alter the data to account for the chirp of the broadband probe pulse. This is because our air- and water-free flow system uses a 2 mm path length sample cell, a distance over which there is significant group velocity mismatch (GVM) between the UV pump pulse and the visible/NIR probe pulses.[28] This GVM effectively limits our time resolution to ∼2 ps, even with our ≤50 fs laser pulses;[29] any additional correction for chirp would be significantly smaller than this. Given the GVM, we do not show any data for delay times less than 5 ps, a time after which the effects of GVM are long over. This means that the price we pay to ensure the purity of our sample is that we lose the earliest time information about the injection kinetics of the excess electron species in liquid CH_3CN; fortunately, Kohler and co-workers have already determined that other than a small ∼2 ps solvation component, there are no significant dynamics in this system on time scales faster than our GVM-limited effective time resolution.[18]

In order to avoid contamination of our acetonitrile sample by water, extra dry, 99.9% pure CH_3CN (≤50 ppm water), stored over molecular sieves, was obtained from Acros Organics and immediately placed in an inert atmosphere glovebox. Iodide solutions were made by dissolving tetrabutylammonium iodide, also obtained from Acros Organics, in the CH_3CN at a 5 mM concentration, except where specified otherwise below. We note that previous experiments on this system used potassium iodide (KI) to make iodide solutions.[18] Our choice to use the tetrabutylammonium cation is based on the fact that it affords greater solubility for the iodide salt; although this was unimportant for the current study, the extra solubility was critical to the performance of 3-pulse experiments that we will describe in future work.[30] We verified that the power dependence of the transient absorption signals we measured was linear, ruling out any possibility of multiphoton excitation of the iodide solution.

RESULTS AND DISCUSSION

As discussed above, the previous study most closely related to our present work is that by Kohler and co-workers, who examined the dynamics of the excess electron species injected into liquid CH_3CN following CTTS excitation of iodide at 266 nm at select probe wavelengths in the visible and NIR.[18] These workers found that the absorption of the NIR species appeared instantaneously and then decayed on three distinct time scales of 1.9, ∼30, and ∼260 ps. The fast, 1.9-ps kinetics were assigned to solvation of the newly injected electron by the solvent. The ∼30 ps decay was only observed only at wavelengths longer than 1300 nm, and was attributed to recombination of the solvated electron with its geminate iodine atom partner. Finally, Kohler and co-workers found that the ∼260 ps decay they observed in the NIR was accompanied by a nearly identical rise at visible probe wavelengths, suggesting that NIR absorbing solvated electrons were disappearing to form solvated dimer anions on this time scale. Thus, these researchers argued that even though the injection kinetics favor formation of the NIR absorbing solvated electron species, there is a subsequent equilibration between solvated electrons solvated molecular anions.[18] Kohler and co-workers also concluded that because the 30 ps time scale they assigned to geminate recombination was seen in the NIR and not in the visible, the kinetics of injection must cause the dimer anion species to form farther away from the parent iodine atom than the solvated electrons.

dx.doi.org/10.1021/jp303591h | J. Phys. Chem. B 2013, 117, 4216−4221

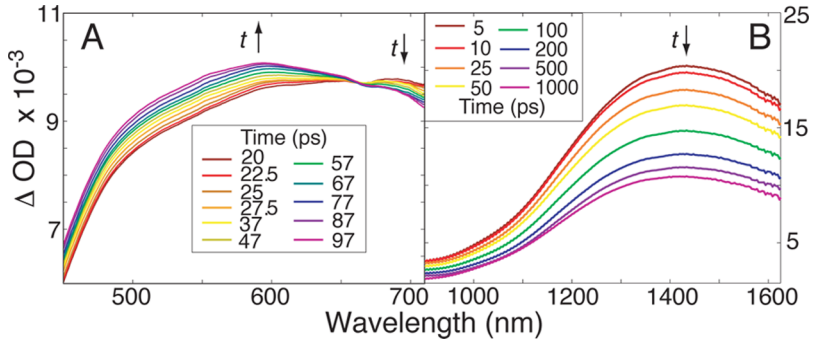

Figure 1. Transient absorption spectra of the excess electron species in liquid CH_3CN created following 266 nm CTTS excitation of iodide and probed in the visible (A) and NIR (B).

To better understand the interconversion and geminate recombination kinetics, we also measured transient absorption spectra of the excess electron species in liquid CH_3CN following CTTS excitation of iodide at 266 nm. Figure 1A shows some of our data in the visible from 450 to 710 nm, a region where both the dimer anion and the (blue tail of the) solvated electron absorb. Over the time window from 20 to 100 ps, the data show that the red portion of the spectrum decays with time, while the blue portion grows with time, with a clear isosbestic point evident at 660 nm. The presence of this well-defined isosbestic point makes it possible to use standard analysis techniques, such as singular value decomposition (SVD), to determine the individual spectra of the two excess electron species in this spectral region. In our analysis, we assumed that the composite spectra we measured had only two underlying components, which interconvert with simple first-order (single-exponential) kinetics. We then used SVD to extract the individual component spectra within this model; the full analysis is described in detail in the Supporting Information, and the results are shown below in Figure 2.

Figure 1B shows our transient absorption spectra of the NIR absorbing CH_3CN solvated electron species at times following the CTTS excitation of I^- from 5 ps to 1 ns. The spectrum we measure is in good agreement with previous work,[16,18,19] and the spectral shape with a peak at ~1430 nm strongly resembles that of solvated electrons in other solvents with similar polarity.[23] The molar extinction coefficient, ε, of this NIR solvated electron band has been previously reported,[16] and the peak value of $\varepsilon_{1430} = 2.4 \times 10^4\ M^{-1}cm^{-1}$ is in accord with other solvents in which the solvated electron absorbs in the same wavelength range. If we use this peak ε for the NIR species and extrapolate the absorption spectrum in the NIR to the visible, the SVD analysis we did for the visible transient absorption spectrum allows us to assign a value for the molar extinction coefficient for the visible-absorbing dimer anion species. We did this by linearly interpolating the NIR spectrum of the solvated electron we measured to the tail of the absorption of this same species extracted from the SVD procedure; this allowed us to assign a cross-section for the blue-tail of the IR-absorbing species. The cross-section of the visible-absorbing species is then strictly determined by the relative amplitudes of the two component spectra extracted from SVD. Our full procedure is described in the Supporting Information, and the results are shown in Figure 2. The figure shows clearly that the absorption cross-section of the dimer anion species (red curve) is intrinsically weak. Based on the low value of the extinction coefficient and the broad, featureless nature of the band, we suspect that this absorption likely results from bound-to-

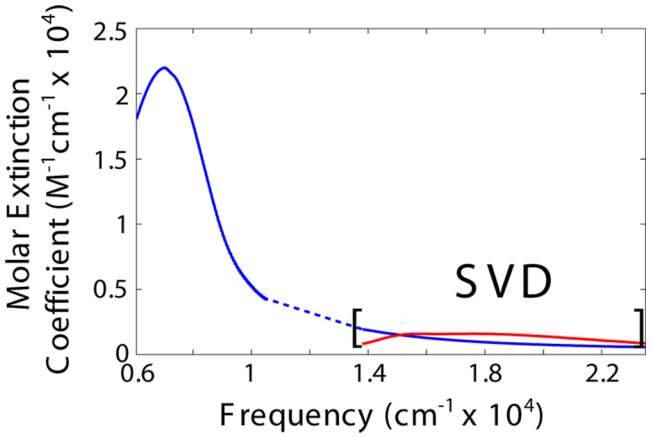

Figure 2. Absolute molar extinction coefficients, ε, for the spectra of the excess electron species in liquid acetonitrile. The high-energy portion of the two spectra were derived via SVD deconvolution from the data in Figure 1. The dotted line represents the linear interpolation used to determined the extinction coefficient of the NIR absorbing solvated electron in the visible region of the spectrum.

continuum transitions. This is in contrast to the large extinction coefficient for the NIR absorbing solvated electron, which, based on work simulating solvated electrons in other polar solvents, likely results from a superposition of bound-to-bound transitions.[31,32] Thus, the low intensity of the visible band does not reflect a low population of dimer anions at equilibrium, but rather, a plentiful species that is simply a poor absorber.

We can quantify the relative amounts of each species present at equilibrium using the individual spectra of each component and molar extinction coefficients shown in Figure 2 to compute the equilibrium constant for the interconversion reaction:

$$K_{eq} = \frac{[\text{dimer anion}]}{[\text{solvated electron}]} \quad (1)$$

where [dimer anion] and [solvated electron] represent the equilibrium concentrations of the two species. If we determine the equilibrium constant using the data in Figure 1 for times after 300 ps, when we are sure the interconversion is complete (as discussed further below and in the Supporting Information), we obtain $K_{eq} = 4.1 \pm 0.2$. This value is quite a bit higher than the 1.3 estimated by Shkrob and Sauer,[19] but to us this higher value makes sense. Nearly all of the previous work on this system via pulsed radiolysis,[16] photoconductivity,[19] and TRPES[26] all conclude that the dimer anion/higher-binding energy species is more stable, suggesting an equilibrium that

dx.doi.org/10.1021/jp303591h | J. Phys. Chem. B 2013, 117, 4216−4221

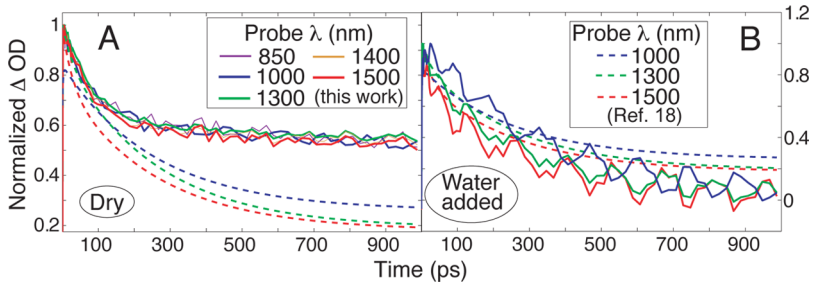

Figure 3. Comparison the NIR spectral kinetics at select wavelengths following electron injection into (A) liquid CH_3CN, and (B) liquid CH_3CN intentionally spiked with a small amount of water, following CTTS excitation of iodide. The solid curves show the data from this study (cf. Figure 1), and the dashed curves are the fits to the data measured by Kohler and co-workers given in ref 18.

favors the dimer anions as opposed to one that is almost balanced. Thus, our results indicate that even though the solvent environment in liquid CH_3CN favors the formation of solvated electrons immediately upon injection, the solvated dimer anion is the more stable of the two species and predominates at equilibrium.

In addition to the clear isosbestic point that allowed us to determine the both absorption cross-section of the solvated CH_3CN dimer anion species and the solvated electron-dimer anion equilibrium constant, the data presented in Figure 1 also show some other differences from the previous work published by Kohler and co-workers.[18] Figure 3A compares NIR single-wavelength transients measured in our experiments with the multiexponential fits to the data for these same wavelengths reported in ref 18. The figure shows clearly that all of the transients measured between 850 and 1500 nm in our experiments are identical within the signal-to-noise, and that the absorption intensity decays by at most 40% of its initial value in the first nanoseconds after electron injection. In contrast, the kinetics reported in ref 18 show distinct differences between the NIR wavelengths, decay more quickly even at the earliest times, and show a total fractional decay of ~80% over the first nanosecond.

We believe that these differences between our results and those of Kohler and co-workers[18] are due to small amounts of water present in the latter's experiments. Liquid acetonitrile is extremely hygroscopic, and exposure of CH_3CN to moisture in the air can easily introduce enough water into the sample to preferentially solvate solutes such as solvated electrons and dimer anions. Such preferential solvation would lead to a dynamic blue-shift of the spectra as the water impurity diffuses to be in the first solvation shell around these solutes.[33] Our suspicion that this took place in the experiments of ref 18 is based on the fact that these workers used a flow jet system for their sample that was open to the air. To verify that water can affect the signals in these experiments, we intentionally spiked our closed-loop sample system with a small amount of liquid water and repeated the experiments; the results are shown in Figure 3B. Clearly, the presence of small amounts of water brings our measurements into agreement with those in ref 18, and also explains why Kohler and co-workers did not observe the clean isosbestic point at 660 nm that is evident in Figure 1A. In the Supporting Information, we also show the complete transient absorption spectra for the sample spiked with small amounts of water; indeed, the dynamic blue-shift due to preferential solvation on a tens of picoseconds time scale[33] is quite evident, in contrast to the water-free data in Figure 1B that show no change in shape on this time scale.

Although we believe that the basic conclusions reached in ref 18—that the injection kinetics favors the solvated electron species and that the two species subsequently equilibrate—are correct, the exact time scales reported in this previous work are likely affected by the presence of water. Thus, to understand the water-free kinetics in this system, we determined the rates of appearance of the visible-absorbing dimer anion and the decay of the NIR absorbing solvated electron using the fitting procedure outlined in the Supporting Information. We found that both the appearance of dimer anions and the decay of solvated electrons were well described by a single exponential function with an 80 ps time constant over the 20 to 100 ps window shown in Figure 1; Figure 4 shows the extracted populations of the two species as well as the single-exponential fit to the early time portion of the data. This equilibration time is significantly faster than the 260 ps reported by Kohler and

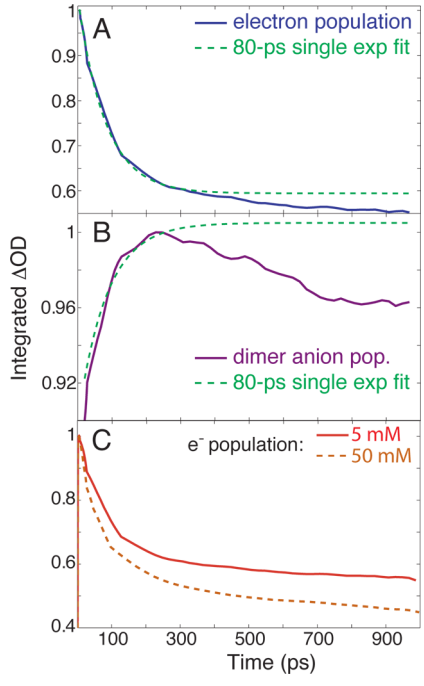

Figure 4. Extracted population decay of the solvated electron (panel A, blue curve) and population rise of the dimer anion (panel B, purple curve) extracted from the data in Figure 1 and fits to a single-exponential interconversion with a time constant of 80 ps (green dashed curves). Extracted population decay of the solvated electron from the NIR transient absorption data for samples at 5 mM (red curve) and 50 mM (orange dashed curve) concentration of iodide (panel C).

dx.doi.org/10.1021/jp303591h | J. Phys. Chem. B 2013, 117, 4216–4221

co-workers,[18] likely because the presence of water in the latter measurements alters the equilibration of the two species. This time is also faster than the 3 ns reported by Shkrob and Sauer, although their experiment had only nanosecond time resolution and would have been unable to measure the 80 ps interconversion rate that we observe.[19]

Another difference between our observations and those in ref 18 concerns the role of geminate recombination of the excess electron species with their geminate iodine atom partners. The fact that we see a clean isosbestic point at times between 20 and 100 ps after the initial injection strongly suggests that no recombination occurs on this time scale. This is because if the two species recombined at different rates, then there would be no isosbestic point, and if they somehow coincidentally recombined at the same rate, the interconversion kinetics would not be single exponential. We do not observe a clean isosbestic point at times earlier than 20 ps, however, which suggests that some process occurs that differentially affects the two species; this process may involve differential solvation or recombination of the two species, but we are hesitant to make a definitive assignment given that our time resolution is limited by GVM. However, we are certain that if recombination is involved, it must be complete within 20 ps and affect at most a few percent of the excess electron population, as discussed in detail in the Supporting Information.

Finally, the data in Figure 1B and Figure 4A,B also show a decay on a time scale of ~600 ps that equally affects both excess electron species. Since this time scale is longer than the 80 ps equilibration time, the natural assignment for a process that removes both species is nongeminate recombination. To verify this assignment, we examined the dependence of the spectral kinetics on the concentration of the iodide salt used for the initial electron injection process. Figure 4C shows that increasing the iodide concentration does not affect the early time kinetics discussed above, but that the long-time decay increases in rate, as would be expected by the presence of additional species with which to recombine. We are unable to determine whether the solvated electrons or solvated dimer anions preferentially recombine, since the loss of either species would lead to a loss of both species due to equilibration on a time scale faster than the nongeminate recombination.

CONCLUDING REMARKS

In summary, we have used air- and water-free techniques to revisit the dynamics of the excess electron species in liquid acetonitrile. In agreement with previous work,[18] we find that the initial injection process preferentially forms solvated electrons, which subsequently interconvert to increase the population of solvated dimer anions. By using broadband ultrafast spectroscopy, we observed a clean isosbestic point during this interconversion process, allowing us to determine that the absorption cross-section of the visible-absorbing dimer anion is significantly smaller than that of the NIR absorbing solvated electron. We also found that the equilibrium favors the dimer anion by a factor of ~4 at room temperature. Analysis of the kinetics of the absorption transients leads us to conclude that geminate recombination, if it occurs, is complete within the first 20 ps and affects only a small fraction of the excess electrons. We find that the time constant for solvated electrons to interconvert into dimer anions is ~80 ps, and that nongeminate recombination occurs on a hundreds of picoseconds time scale, depending on the concentration. It is well established that preferential solvation by small amounts of water can affect both the transient spectral dynamics and recombination kinetics of solvated electrons,[33] and we believe that small amounts of water in highly hygroscopic CH_3CN that has been exposed to air can explain the differences in our data relative to those in previous work.[18] With the cross sections and population dynamics now established, we will turn in future work to performing pump−probe studies on the equilibrated excess electron species in liquid acetonitrile to better understand the details of how these two species are interconnected and the reasons why the solvated electron is favored kinetically but not thermodynamically.[30]

ASSOCIATED CONTENT

Supporting Information

Data analysis including SVD deconvolution, spectral fitting and extraction of dynamic populations, and determination of the equilibrium constant. This material is available free of charge via the Internet at http://pubs.acs.org/.

AUTHOR INFORMATION

Corresponding Author

*E-mail: schwartz@chem.ucla.edu.

Notes

The authors declare no competing financial interest.

ACKNOWLEDGMENTS

This work was supported by the National Science Foundation under grant numbers CHE-0741804 and CHE-0908548.

REFERENCES

(1) Long, F. H.; Lu, H.; Shi, X.; Eisenthal, K. B. *Chem. Phys. Lett.* **1990**, *169*, 165−171.
(2) Kimura, Y.; Alfano, J. C.; Walhout, P. K.; Barbara, P. F. *J. Phys. Chem.* **1994**, *98*, 3450−3458.
(3) Silva, C.; Walhout, P. K.; Yokoyama, K.; Barbara, P. F. *Phys. Rev. Lett.* **1998**, *80*, 1086−1089.
(4) Kloepfer, J. A.; Vilchiz, V. H.; Lenchenkov, V. A.; Bradforth, S. E. *Chem. Phys. Lett.* **1998**, *298*, 120−128.
(5) Hart, E. J.; Boag, J. W. *J. Am. Chem. Soc.* **1962**, *84*, 4090−4095.
(6) Sprik, M.; Impey, R. W.; Klein, M. L. *J. Chem. Phys.* **1985**, *83*, 5802−5809.
(7) Sprik, M.; Impey, R. W.; L., K. M. *J. Stat. Phys.* **1986**, *43*, 967−972.
(8) Staib, A.; Borgis, D. *J. Chem. Phys.* **1996**, *104*, 9027−9039.
(9) Kloepfer, J. A.; Vilchiz, V. H.; Lenchenkov, V. A.; Germaine, A. C.; Bradforth, S. E. *J. Chem. Phys.* **2000**, *113*, 6288−6307.
(10) Vilchiz, V. H.; Kloepfer, J. A.; Germaine, A. C.; Lenchenkov, V. A.; Bradforth, S. E. *J. Phys. Chem. A* **2001**, *105*, 1711−1723.
(11) Vilchiz, V. H.; Chen, X.; Kloepfer, J. A.; Bradforth, S. E. *Radiat. Phys. Chem.* **2005**, *72*, 159−167.
(12) Rosenthal, S. J.; Xie, X.; Du, M.; Fleming, G. R. *J. Chem. Phys.* **1991**, *95*, 4715.
(13) Maroncelli, M. *J. Chem. Phys.* **1991**, *94*, 2084.
(14) Roy, S.; Komath, S.; Bagchi, B. *J. Chem. Phys.* **1993**, *99*, 3139.
(15) Ladanyi, B. M.; Klein, S. *J. Chem. Phys.* **1996**, *105*, 1552.
(16) Bell, I. P.; Rodgers, M. A. J.; Burrows, H. D. *J. Chem. Soc.* **1976**, 315−326.
(17) Mulac, W. A.; Bromberg, A.; Meisel, D. *Radiat. Phys. Chem.* **1985**, *26*, 205−209.
(18) Xia, C.; Peon, J.; Kohler, B. *J. Chem. Phys.* **2002**, *117*, 8855−8866.
(19) Shkrob, I. A.; Sauer, M. C., Jr. *J. Phys. Chem. A* **2002**, *106*, 9120−9131.
(20) Mitsui, M.; Ando, N.; Kokubo, S.; Nakajima, A.; Kaya, K. *Phys. Rev. Lett.* **2003**, *91*, 153002.

(21) Takayanagi, T.; Hoshino, T.; Takahashi, K. *Chem. Phys.* **2006**, *324*, 679−688.
(22) Timerghazin, Q. K.; Peslherbe, G. H. *J. Phys. Chem. B* **2008**, *112*, 520−528.
(23) Fox, M. F.; Hayon, E. *Chem. Phys. Lett.* **1972**, *14*, 442−444.
(24) Ehrler, O. T.; Griffin, G. B.; Young, R. M.; Neumark, D. M. *J. Phys. Chem. B* **2009**, *113*, 4031−4037.
(25) Ehrler, O. T.; Neumark, D. M. *Acc. Chem. Res.* **2009**, *42*, 769−777.
(26) Young, R. M.; Griffin, G. B.; Kammrath, A.; Ehrler, O. T.; Neumark, D. M. *Chem. Phys. Lett.* **2010**, *485*, 59−63.
(27) Bragg, A. E.; Glover, W. J.; Schwartz, B. J. *Phys. Rev. Lett.* **2010**, *104*, 233005.
(28) Kozma, I. Z.; Krok, P.; Reidle, E. *J. Opt. Soc. Am. B* **2005**, *22*, 1479−1485.
(29) Bragg, A. E.; Schwartz, B. J. *J. Phys. Chem. A* **2008**, *112*, 3530.
(30) Doan, S. C.; Schwartz, B. J. Manuscript in preparation, 2012.
(31) Schwartz, B. J.; Rossky, P. J. *J. Chem. Phys.* **1994**, *101*, 6902.
(32) Turi, L.; Mosyak, A.; Rossky, P. J. *J. Chem. Phys.* **1997**, *107*, 1970.
(33) Bragg, A. E.; Kanu, G. U.; Schwartz, B. J. *J. Phys. Chem. Lett.* **2011**, *2*, 2797.